

PROPAGATION OF LAMB WAVES AND SH WAVES IN BONDED PLATES

Silvio de Barros

Université de Versailles Saint-Quentin-en-Yvelines – LEMA, RC 28 - Bat Descartes 78025 Versailles FRANCE
silvio.debarros@meca.uvsq.fr

Antonio Lopes Gama

Universidade Federal Fluminense, Dep. de Engenharia Mecânica 24210-000, Niterói, RJ, Brasil
agama@mec.uff.br

Martine Rousseau

Université Paris VI - LMM CNRS UMR 7607
mrousse@moka.ccr.jussieu.fr

Bernard Collet

Université Paris VI - LMM CNRS UMR 7607
bc@ccr.jussieu.fr

Abstract. In this paper the propagation of guided Lamb waves and guided shear horizontally polarized (SH) waves in bonded plates is investigated. A model based on distributions of springs (quasi-static approximation) is used to describe the interaction of guided waves with imperfect adhesive layers. Through this approach, the imperfections of the adhesive layer were reproduced by changing the stiffness constant of the springs. The wave dispersion spectra for the Lamb waves and SH waves was obtained for different conditions of the adhesive layer. The results show that Lamb waves and the SH waves are sensitive to the alterations of the adhesive layer and have a great potential for the evaluation of bonded joints.

Keywords. Bonded joints, Lamb waves, SH waves.

1. Introduction

The need for increasing structural performance, with low weight and high strength, has demanded the use of more effective joining methodologies. Mainly due to their low weight, low cost and ease of assembly, the adhesive bonds have emerged as a promising technology (Heller *et al.*, 2000). The widespread use of adhesive joints is also indicative of the advantages of the adhesive bonding over techniques such as welding and riveting.

However, the use of adhesive bonding in aircraft structures and other safety critical applications has been limited due to the lack of adequate nondestructive testing procedures. Defects such as disbonds, voids and porosity; weak bond between the adhesive layer and adherent and a weak adhesive layer are commonly found in adhesive layers (Guyott and Cawley, 1988).

The great expansion of the use of bonded joints and bonded repairs has motivated the development of more reliable nondestructive methodologies. The conventional ultrasonic techniques, based on the echoes reflected by the defects, are not effective for inspection of most practical bonded joints due to the small thickness of the adhesive layer. In this case, the ultrasonic waves reflected by the interfaces of the adhesive layer are not separated in the time domain and interfere (Lavrentyev and Rokhlin, 1998). Also the conventional ultrasonic techniques are ineffective in interrogating large bonded areas. New methodologies using guided waves have been investigated for the inspection of bonded components. The primary advantage of using guided waves is that they can interrogate large areas, they also have many modes of propagation that can be selected accordingly with the objective of the analysis (Maslov and Kundu, 1997 and Kundu and Maslov, 1997).

In this paper, the propagation of guided Lamb waves and guided shear horizontally polarized waves (SH) in bonded plates is investigated. The quasi-static approximation (QSA) was used to describe the interaction of guided waves with imperfect adhesive layers. This model is based on the continuous distribution of springs to represent the adhesive layer. Through this approach, the imperfections of the adhesive layer can be reproduced by changing the stiffness constants of the springs (Pecorari and Kelly, 2000; Singher *et al.*, 1994; Xu, P.C., and Datta, S.K., 1990). The wave dispersion spectra for the Lamb waves and SH waves was obtained for different conditions of the adhesive layer. The results shown that ultrasonic guided waves have a great potential for the evaluation of bonded joints.

2. Propagation of Lamb waves and SH waves in a homogeneous infinite plate

The basic concepts of wave propagation will be introduced through the analysis of Lamb waves propagation in a homogeneous infinite plate, as shown in Fig. (1) (Achenbach, 1975 and Graff, 1991). We consider a plane strain state in the xz plane and consequently the propagation of longitudinal (P) and transverse (SV) waves.

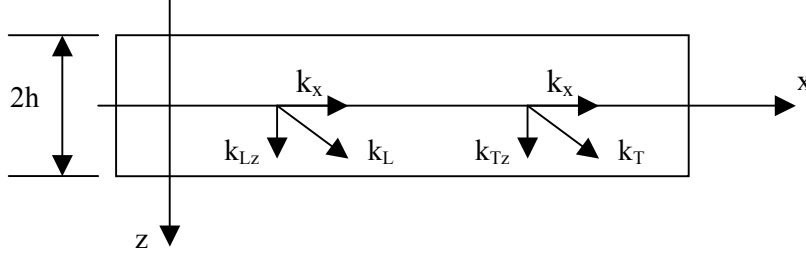


Figure 1. Infinite plate of thickness $2h$.

For a homogeneous isotropic plate, the displacement equations of motion can be written as:

$$\mu \nabla^2 \mathbf{u} + (\lambda + \mu) \nabla \nabla \cdot \mathbf{u} = \rho \ddot{\mathbf{u}} \quad (1)$$

where λ and μ are the Lamé's coefficients. Using the Helmholtz's decomposition, we can write the displacements in the following form:

$$\mathbf{u} = \nabla \phi + \nabla \wedge \psi \quad (2)$$

where ϕ is a scalar potential and ψ is a vector potential, with the constraint condition $\nabla \cdot \psi = 0$.

For a time-harmonic wave motion and grouping the symmetric and anti-symmetric components, the scalar and vector potentials can be expressed as:

$$\begin{aligned} \phi &= [S_L \cos(k_{Lz}z) + A_L \text{sen}(k_{Lz}z)] e^{i(k_x x - \omega t)} \\ \psi &= [A_T \cos(k_{Tz}z) + S_T \text{sen}(k_{Tz}z)] e^{i(k_x x - \omega t)} \end{aligned} \quad (3)$$

where K_x and K_{Lz} are the components of the longitudinal wave number vector and K_x and K_{Tz} are the components of the transverse wave number vector. S and A represent the symmetric and anti-symmetric components. L and T refer to the components of longitudinal and transverse waves respectively. The components of the displacement vector \mathbf{u} can be determined substituting Eq. (3) in Eq. (2):

$$\begin{aligned} u_x &= [ik_x S_L \cos(k_{Lz}z) + ik_x A_L \text{sen}(k_{Lz}z) + k_{Tz} A_T \text{sen}(k_{Tz}z) - k_{Tz} S_T \cos(k_{Tz}z)] e^{i(k_x x - \omega t)} \\ u_z &= [-k_{Lz} S_L \text{sen}(k_{Lz}z) + k_{Lz} A_L \cos(k_{Lz}z) + ik_x A_T \cos(k_{Tz}z) + ik_x S_T \text{sen}(k_{Tz}z)] e^{i(k_x x - \omega t)} \end{aligned} \quad (4)$$

Using the Hooke's law, the stress components can be given by:

$$\begin{aligned} \sigma_{xz} &= \mu \left[-2ik_{Lz} k_x S_L \text{sen}(k_{Lz}z) + S_T (k_T^2 - 2k_x^2) \text{sen}(k_{Tz}z) + \right. \\ &\quad \left. + 2ik_{Lz} k_x A_L \cos(k_{Lz}z) + A_T (k_T^2 - 2k_x^2) \cos(k_{Tz}z) \right] e^{i(k_x x - \omega t)} \\ \sigma_{zz} &= \mu \left[- (k_T^2 - 2k_x^2) S_L \cos(k_{Lz}z) + 2ik_{Tz} k_x S_T \cos(k_{Tz}z) + \right. \\ &\quad \left. - (k_T^2 - 2k_x^2) A_L \text{sen}(k_{Lz}z) - 2ik_{Tz} k_x A_T \text{sen}(k_{Tz}z) \right] e^{i(k_x x - \omega t)} \end{aligned} \quad (5)$$

The boundary conditions for the free surfaces of the plate are:

$$\begin{aligned} \sigma_{xz} &= 0 \Rightarrow z = \pm h \forall x, t \\ \sigma_{zz} &= 0 \Rightarrow z = \pm h \forall x, t \end{aligned} \quad (6)$$

Applying the boundary conditions in Eq. (5), we can find a system of equations that will be decomposed in two systems: one for the symmetric and the other for the anti-symmetric modes.

For the symmetric modes we obtain:

$$\begin{bmatrix} -2ik_{Lz}k_x \text{sen}(k_{Lz}h) & (k_T^2 - 2k_x^2)\text{sen}(k_{Tz}h) \\ -(k_T^2 - 2k_x^2)\text{cos}(k_{Lz}h) & 2ik_{Tz}k_x \text{cos}(k_{Tz}h) \end{bmatrix} \begin{Bmatrix} S_L \\ S_T \end{Bmatrix} = \begin{Bmatrix} 0 \\ 0 \end{Bmatrix} \quad (7)$$

and for the anti-symmetric modes:

$$\begin{bmatrix} 2ik_{Lz}k_x \text{cos}(k_{Lz}h) & (k_T^2 - 2k_x^2)\text{cos}(k_{Tz}h) \\ (k_T^2 - 2k_x^2)\text{sen}(k_{Lz}h) & 2ik_{Tz}k_x \text{sen}(k_{Tz}h) \end{bmatrix} \begin{Bmatrix} A_L \\ A_T \end{Bmatrix} = \begin{Bmatrix} 0 \\ 0 \end{Bmatrix} \quad (8)$$

Figure (2) shows the frequency spectrum for an aluminum plate ($E = 71 \times 10^9$ MPa e $\nu = 0,3$), where $\Omega = \omega h / C_T$ and $\xi = k_x h$ are the dimensionless frequency and dimensionless wave number, respectively. The branches shown in Figure (2) correspond to the non-trivial solutions of Eq. (7) and Eq. (8).

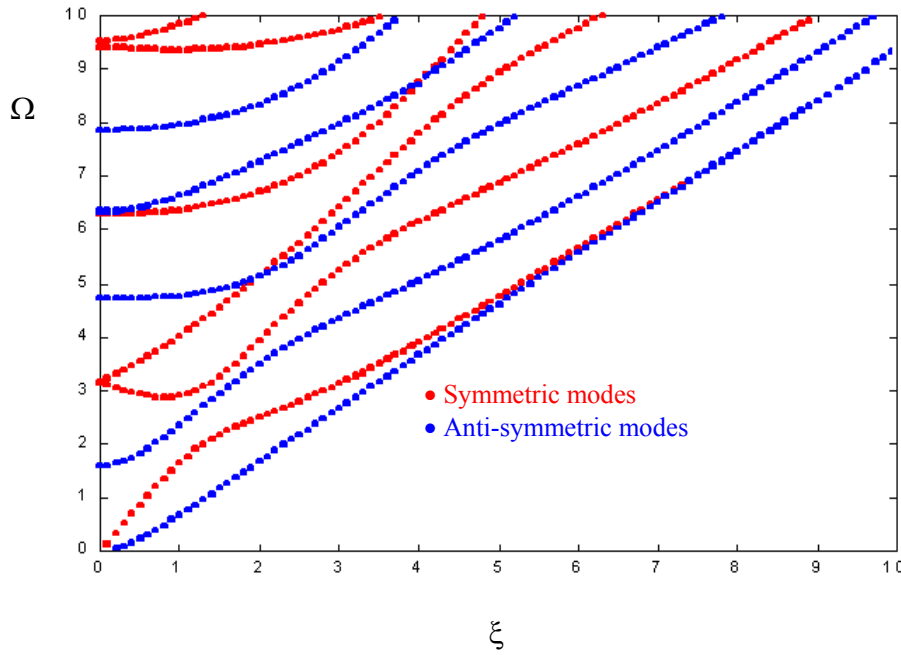


Figure 2. Frequency spectrum for Lamb waves in an aluminum plate.

Due to the lack of space the details to obtain the frequency equation for SH waves will be omitted here. The complete procedure can be found in Achenbach, J.D., 1975.

The SH waves have displacement components in the y direction only. For a time-harmonic wave motion the displacement in the y direction can be written in the form:

$$u_y = A(z)e^{i(kx - \omega t)} \quad (9)$$

In the Ω - ξ plane the frequency equation for SH-modes can be given by:

$$\Omega^2 = \xi^2 + n^2\pi^2 \quad (10)$$

The frequency spectrum for the SH-modes in an aluminum plate is shown in Fig. (3).

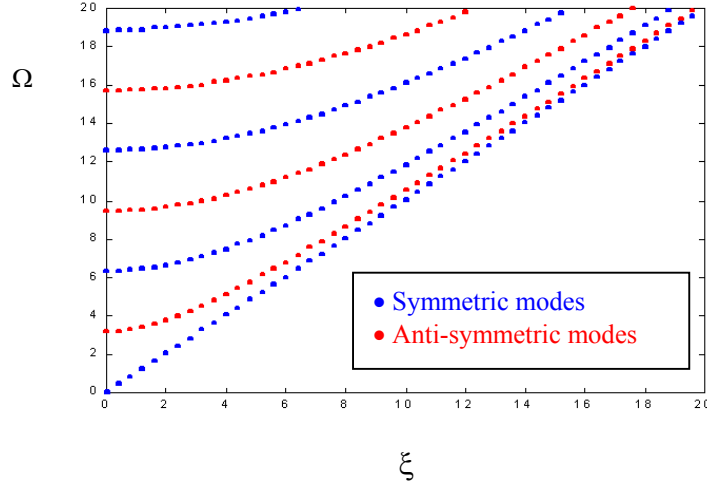


Figure 3. Frequency spectrum for SH waves in an aluminum plate.

3. Propagation of Lamb waves in bonded plates

In this section a model based on the continuous distribution of springs is used to describe the adhesive layer as shown in Fig. (4). This procedure is known as the quasi-static approximation (QSA) (Baik, and Thompson, 1984). Through this approach the defects of the adhesive layer can be simulated changing the stiffness constants of the springs (Pecorari, and Kelly, 2000; Singher, et al., 1994; Xu, and Datta, 1990 and de Barros, 2001).

The objective of this section is to investigate the propagation of Lamb waves in two bonded plates for different conditions of the adhesive layer.

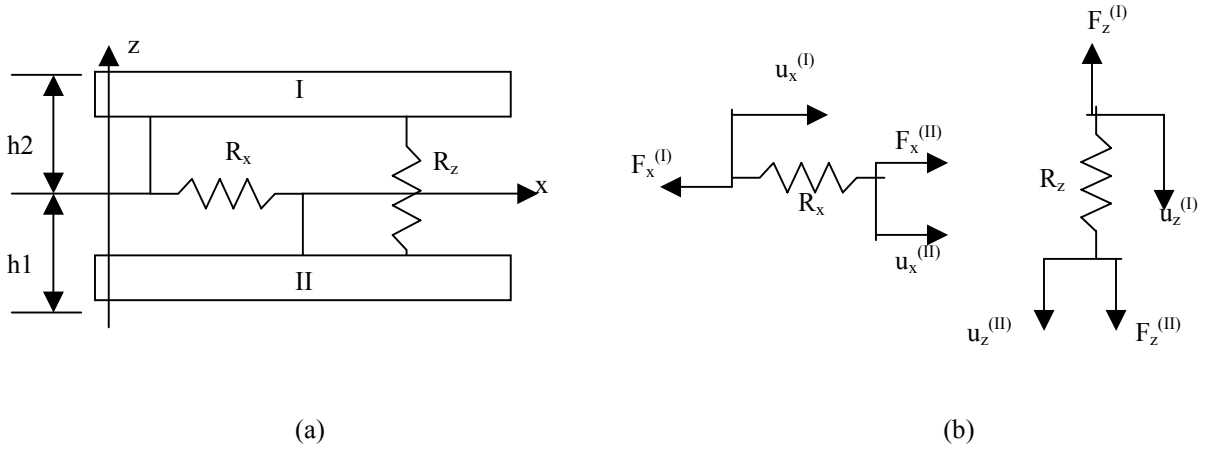


Figure 4. Model of the adhesive layer (a) and forces on the springs (b).

Applying the boundary conditions given by Eqs. (6), in Eqs. (5), for the free surface of plate I and plate II, we obtain the following equations:

$$2ik_{Lz}k_x \text{sen}(k_{Lz}h_1)S_L^{(I)} - (k_T^2 - 2k_x^2)\text{sen}(k_{Tz}h_1)S_T^{(I)} + 2ik_{Lz}k_x \cos(k_{Lz}h_1)A_L^{(I)} + (k_T^2 - 2k_x^2)\cos(k_{Tz}h_1)A_T^{(I)} = 0 \quad (11)$$

$$-(k_T^2 - 2k_x^2)\cos(k_{Lz}h_1)S_L^{(I)} + 2ik_{Tz}k_x \cos(k_{Tz}h_1)S_T^{(I)} + (k_T^2 - 2k_x^2)\text{sen}(k_{Lz}h_1)A_L^{(I)} + 2ik_{Tz}k_x \text{sen}(k_{Tz}h_1)A_T^{(I)} = 0 \quad (12)$$

$$-2ik_{Lz}k_x \text{sen}(k_{Lz}h_2)S_L^{(II)} + (k_T^2 - 2k_x^2)\text{sen}(k_{Tz}h_2)S_T^{(II)} + 2ik_{Lz}k_x \cos(k_{Lz}h_2)A_L^{(II)} + (k_T^2 - 2k_x^2)\cos(k_{Tz}h_2)A_T^{(II)} = 0 \quad (13)$$

$$\begin{aligned}
& -\left(k_T^2 - 2k_x^2\right)\cos(k_{Lz}h_2)S_L^{(II)} + 2ik_{Tz}k_x \cos(k_{Tz}h_2)S_T^{(II)} - \left(k_T^2 - 2k_x^2\right)\text{sen}(k_{Lz}h_2)A_L^{(II)} + \\
& - 2ik_{Tz}k_x\text{sen}(k_{Tz}h_2)A_T^{(II)} = 0
\end{aligned} \tag{14}$$

The boundary conditions in the adhesive layer can be written as:

$$\sigma_{xz}^{(I)} = \hat{R}x(u_x^{(II)} - u_x^{(I)}) \tag{15}$$

$$\sigma_{zz}^{(I)} = \hat{R}z(u_z^{(II)} - u_z^{(I)}) \tag{16}$$

$$\sigma_{xz}^{(II)}\Big|_{z=0^-} = \sigma_{xz}^{(I)}\Big|_{z=0^+} \tag{17}$$

$$\sigma_{zz}^{(II)}\Big|_{z=0^-} = \sigma_{zz}^{(I)}\Big|_{z=0^+} \tag{18}$$

where $\hat{R}x = \frac{Rx}{S}$ and $\hat{R}z = \frac{Rz}{S}$. S is the area of the adhesive layer in the plane xy.

Using the Eqs. (4) and (5) for $z = 0$, the expressions for the displacements and stresses on the interfaces can be given by:

$$u_x^{(I)}\Big|_{z=0} = [iS_L^{(I)}k_x - S_T^{(I)}k_{Tz}]e^{i(k_x x - \omega t)} \tag{19}$$

$$u_z^{(I)}\Big|_{z=0} = [A_L^{(I)}k_{Lz} + iA_T^{(I)}k_x]e^{i(k_x x - \omega t)} \tag{20}$$

$$u_x^{(II)}\Big|_{z=0} = [iS_L^{(II)}k_x - S_T^{(II)}k_{Tz}]e^{i(k_x x - \omega t)} \tag{21}$$

$$u_z^{(II)}\Big|_{z=0} = [A_L^{(II)}k_{Lz} + iA_T^{(II)}k_x]e^{i(k_x x - \omega t)} \tag{22}$$

$$\sigma_{xz}^{(I)}\Big|_{z=0^-} = \mu[2iA_L^{(I)}k_{Lz}k_x + A_T^{(I)}(k_T^2 - 2k_x^2)]e^{i(k_x x - \omega t)} \tag{23}$$

$$\sigma_{zz}^{(I)}\Big|_{z=0^-} = \mu[-S_L^{(I)}(k_T^2 - 2k_x^2) + 2iS_T^{(I)}k_{Tz}k_x]e^{i(k_x x - \omega t)} \tag{24}$$

$$\sigma_{xz}^{(II)}\Big|_{z=0^+} = \mu[2iA_L^{(II)}k_{Lz}k_x + A_T^{(II)}(k_T^2 - 2k_x^2)]e^{i(k_x x - \omega t)} \tag{25}$$

$$\sigma_{zz}^{(II)}\Big|_{z=0^+} = \mu[-S_L^{(II)}(k_T^2 - 2k_x^2) + 2iS_T^{(II)}k_{Tz}k_x]e^{i(k_x x - \omega t)} \tag{26}$$

By applying Eqs. (19) to (26) in Eqs. (15) to (18) we obtain the following equations:

$$ik_x S_L^{(I)} - k_{Tz} S_T^{(I)} - ik_x S_L^{(II)} + k_{Tz} S_T^{(II)} + \frac{\mu}{\hat{R}x} 2ik_{Lz} k_x A_L^{(II)} + \frac{\mu}{\hat{R}x} (k_T^2 - 2k_x^2) A_T^{(II)} = 0 \tag{27}$$

$$k_{Lz} A_L^{(I)} + ik_x A_T^{(I)} - \frac{\mu}{\hat{R}z} (k_T^2 - 2k_x^2) S_L^{(II)} + \frac{\mu}{\hat{R}z} 2ik_{Tz} k_x S_T^{(II)} - k_{Lz} A_L^{(II)} - ik_x A_T^{(II)} = 0 \tag{28}$$

$$2iA_L^{(I)}k_{Lz}k_x + A_T^{(I)}(k_T^2 - 2k_x^2) - 2iA_L^{(II)}k_{Lz}k_x - A_T^{(II)}(k_T^2 - 2k_x^2) = 0 \tag{29}$$

$$-S_L^{(I)}(k_T^2 - 2k_x^2) + 2iS_T^{(I)}k_{Tz}k_x + S_L^{(II)}(k_T^2 - 2k_x^2) - 2iS_T^{(II)}k_{Tz}k_x = 0 \tag{30}$$

The solutions of the system of Eqs. (11) to (14) and Eqs. (27) to (30) constitutes the frequency spectrum for the Lamb waves in the two bonded plates.

3.1 Dispersion curves of Lamb waves in bonded plates

The dispersion curves of Lamb waves was obtained for different conditions of the adhesive layer. First the perfect adhesion was simulated by assuming very high values for $\hat{R}x$ and $\hat{R}z$. In this case the stiffness of the adhesive layer is considered infinite. For this condition, the dispersion curves for the aluminum bonded plates was compared with the dispersion curves for a single aluminum plate of thickness 2h and the results shown an excellent agreement. We concluded that the stiffness of 1×10^{17} N/m³ for $\hat{R}x$ and $\hat{R}z$ can represent the case of a perfect adhesion for the two bonded aluminum plates. Next, the stiffness of the springs was gradually reduced to simulate deficient conditions of the

adhesive layer. Figures (5) and (6) show the dispersion curves for $\widehat{R}x = 10^{15} \text{ N/m}^3$ and $\widehat{R}z = 1 \times 10^{17} \text{ N/m}^3$, and the dispersion curves for $\widehat{R}x = 10^{17} \text{ N/m}^3$ and $\widehat{R}z = 1 \times 10^{15} \text{ N/m}^3$, respectively. For both cases the results are compared with the ideal condition of adhesion ($\widehat{R}x = \widehat{R}z = 1 \times 10^{17} \text{ N/m}^3$).

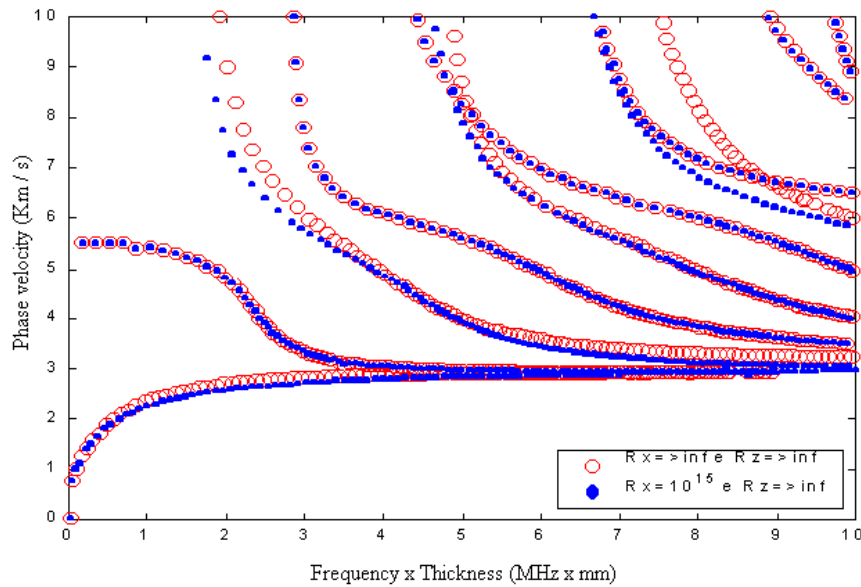


Figure 5. Dispersion curves for $\widehat{R}x = 10^{15} \text{ N/m}^3$ and $\widehat{R}z = 1 \times 10^{17} \text{ N/m}^3$ (blue), and dispersion curves for $\widehat{R}x = 10^{17} \text{ N/m}^3$ and $\widehat{R}z = 1 \times 10^{17} \text{ N/m}^3$ (red).

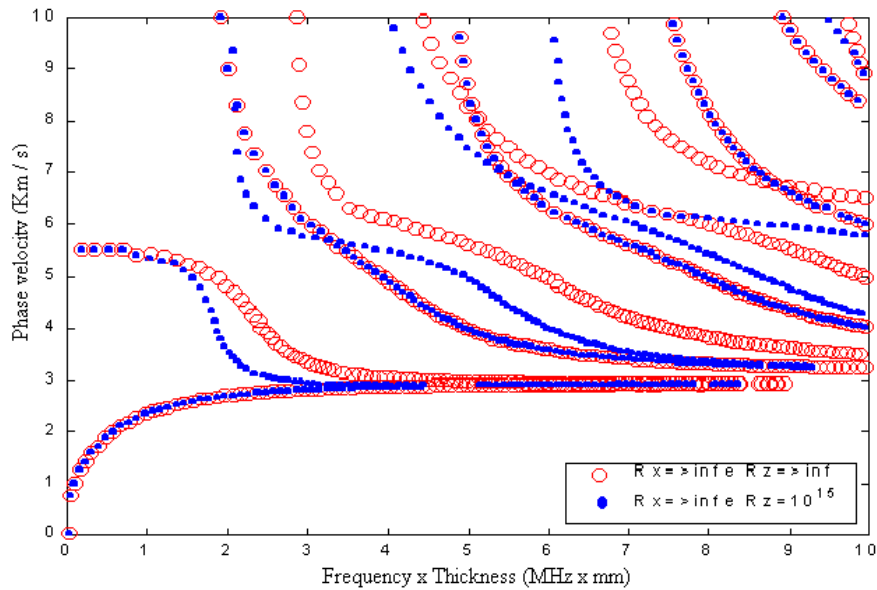


Figure 6. Dispersion curves for $\widehat{R}x = 10^{17} \text{ N/m}^3$ and $\widehat{R}z = 1 \times 10^{15} \text{ N/m}^3$ (blue), and dispersion curves for $\widehat{R}x = 10^{17} \text{ N/m}^3$ and $\widehat{R}z = 1 \times 10^{17} \text{ N/m}^3$ (red).

The dispersion curves of Fig. (5) and Fig. (6) show that only the anti-symmetric modes change when reducing $\widehat{R}x$ and only the symmetric modes change when reducing $\widehat{R}z$. This can also be concluded regarding Eq. (4) for $z = 0$, where for the symmetric modes, the symmetric part of u_x is zero and for the anti-symmetric modes, the anti-symmetric part of u_z is zero.

The phase velocity in function of $\widehat{R}x$ for the first anti-symmetric mode A0 is shown in detail in Fig. (7) (a), while the Fig. (7) (b) shows the phase velocity for the first symmetric mode S0 in function of $\widehat{R}z$. Accordingly with Figs. (7), the phase velocity for both modes decrease due to the reduction of the stiffness of the adhesive layer.

We observed that the Lamb wave modes are sensitive to the alterations of the adhesive layer and that the general condition of the adhesive layer can be described by monitoring the propagation of Lamb waves. Recent ultrasonic

techniques using guided waves are able to excite only some Lamb wave modes (Monkhouse, *et al.*, 1998). Also, as reported by Heller, *et al.*, 2000 and Mustafa, *et al.*, 1997, variations of the phase velocity of Lamb waves can be used to evaluate the conditions of the adhesive layer.

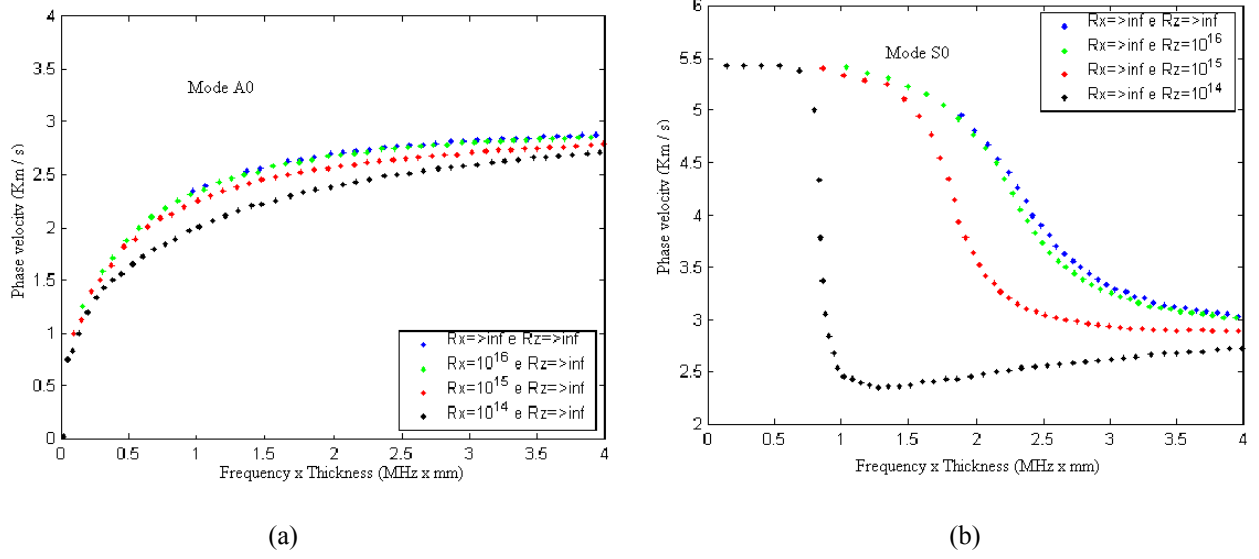


Figure 7. Phase velocity of mode A0 (a) and mode S0 (b) due to the reduction of the spring stiffness.

4. Propagation of SH waves in bonded plates

In this section, the quasi-static approximation is also used to simulate the propagation of SH waves in aluminum bonded plates, as shown in Fig. (8). The SH waves have displacement components in the y direction and consequently, only the springs in the y direction are considered.

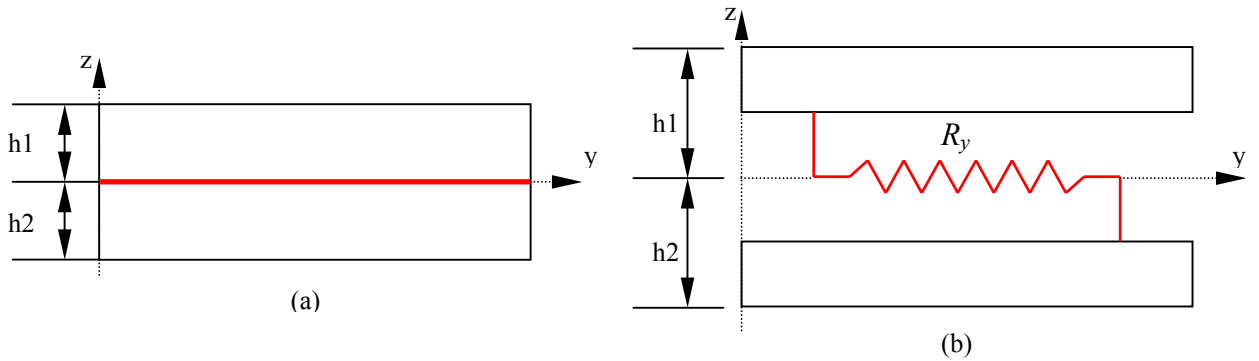


Figure 8. Model of the adhesive layer to simulate the propagation of SH waves in bonded plates.

As for the case of a single plate (Achenbach, J.D., 1975), the displacement u_y for each plate can be given by:

$$\begin{cases} u_y^{(I)} &= [B_1 \cos(K_{T_2} z) + B_2 \sin(K_{T_2} z)] e^{i(K_1 x - \omega t)} \\ u_y^{(II)} &= [B_3 \cos(K_{T_3} z) + B_4 \sin(K_{T_3} z)] e^{i(K_1 x - \omega t)} \end{cases} \quad (31)$$

where $K_{T_2}^2 = \frac{\omega^2}{C_T^2} - K_1^2$. Using the Hookes' law, we can find that :

$$\sigma_{yz} = \mu u_{y,z} \quad (32)$$

Applying the boundary conditions $\sigma_{xz} = \sigma_{yz} = \sigma_{zz} = 0$, for the free surfaces $z = h_1$ and $z = -h_2$:

$$u_{y,z}^{(I)} \Big|_{z=h_1} = 0 \text{ and } u_{y,z}^{(II)} \Big|_{z=-h_2} = 0 \quad (33)$$

Next, applying the conditions given by Eq. (33) in Eq. (31), we can find the following equations:

$$\begin{aligned} -B_1 \text{sen}(K_{Tz} h_1) + B_2 \cos(K_{Tz} h_1) &= 0 \\ B_3 \text{sen}(K_{Tz} h_2) + B_4 \cos(K_{Tz} h_2) &= 0 \end{aligned} \quad (34)$$

The boundary conditions in the adhesive layer can be written as:

$$\sigma_{yz}^{(I)} = -\widehat{R}_y (u_y^{(II)} - u_y^{(I)}) \quad (35)$$

$$\sigma_{yz}^{(I)} = \sigma_{yz}^{(II)} \Rightarrow \mu u_{y,z}^{(I)} = \mu u_{y,z}^{(II)} \Rightarrow u_{y,z}^{(I)} = u_{y,z}^{(II)} \quad (36)$$

$$\text{where } \widehat{R}_y = \frac{R_y}{S}.$$

Applying Eq. (36) in Eqs. (31) for $z = 0$, we find that:

$$B_2 - B_4 = 0 \quad (37)$$

Using Eq. (32), Eq. (35), and Eq. (31), we obtain:

$$-\widehat{R}_y B_1 + \mu K_{Tz} B_2 + \widehat{R}_y B_3 = 0 \quad (38)$$

Equations (34), (37) and (38) may be rewritten in matrix form:

$$\underbrace{\begin{bmatrix} -\text{sen}(K_{Tz} h_1) & \cos(K_{Tz} h_1) & 0 & 0 \\ 0 & 0 & \text{sen}(K_{Tz} h_2) & \cos(K_{Tz} h_2) \\ -\widehat{R}_y & \mu K_{Tz} & \widehat{R}_y & 0 \\ 0 & 1 & 0 & -1 \end{bmatrix}}_{\mathbf{F}} \underbrace{\begin{Bmatrix} B_1 \\ B_2 \\ B_3 \\ B_4 \end{Bmatrix}}_{\mathbf{b}} = \begin{Bmatrix} 0 \\ 0 \\ 0 \\ 0 \end{Bmatrix} \quad (39)$$

The determinant of \mathbf{F} must vanish, which yields the following equation:

$$\text{sen} \left[(\Omega^2 - \xi^2)^{1/2} \right] - \frac{\mu}{h \widehat{R}_y} (\Omega^2 - \xi^2)^{1/2} \text{sen} \left[\varepsilon_1 (\Omega^2 - \xi^2)^{1/2} \right] \text{sen} \left[\varepsilon_2 (\Omega^2 - \xi^2)^{1/2} \right] = 0 \quad (40)$$

$$\text{where: } \varepsilon_1 = \frac{h_1}{h} \text{ and } \varepsilon_2 = \frac{h_2}{h}.$$

4.1 Dispersion curves of SH waves in bonded plates

The same procedure used to investigate the propagation of Lamb waves in bonded plates, as described in section 3, was applied here to study the propagation of SH waves. The frequency spectrum of SH waves was also obtained for different conditions of the adhesive layer, using Eq. (40), beginning with the perfect adhesion ($\widehat{R}_y = 1 \times 10^{17} \text{ N/m}^3$) and gradually decreasing the stiffness of the spring to simulate deficient conditions of the adhesive layer. Figure (9) shows the frequency spectrum of SH waves for different stiffness constant \widehat{R}_y . Note that only the branches of the anti-symmetric modes change and become closer to the branches of the symmetric modes for low \widehat{R}_y . Figure (10) show the phase velocity curves for the first anti-symmetric mode for different stiffness constant \widehat{R}_y .

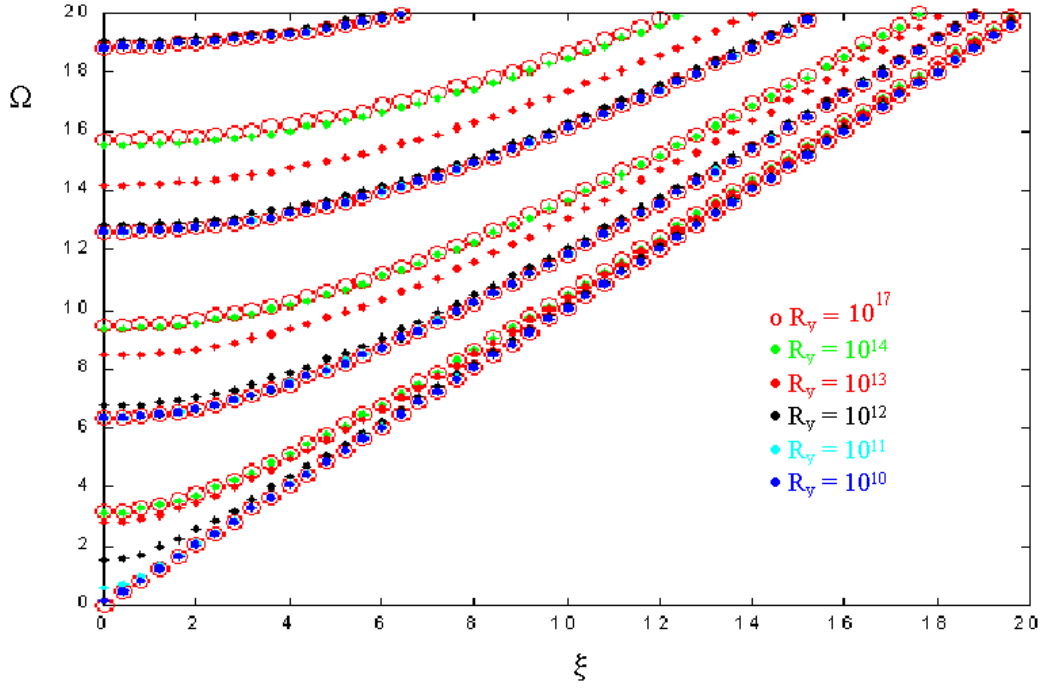


Figure 9. Frequency spectrum of SH waves for different stiffness constant \widehat{R}_y .

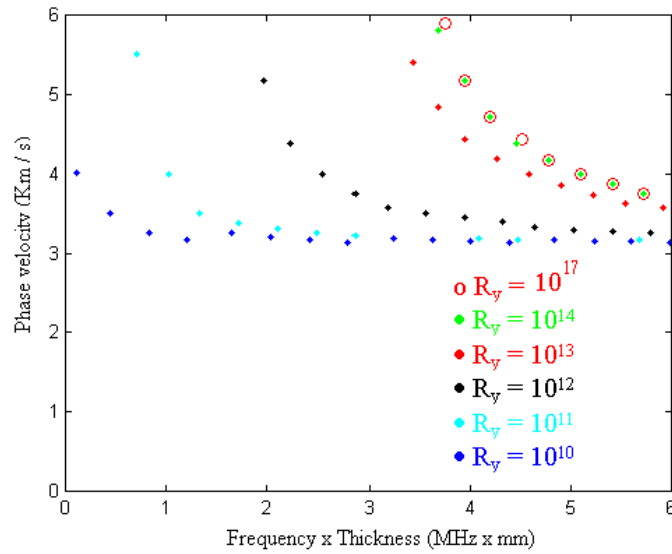


Figure 10. Phase velocity curves for the first anti-symmetric mode for different stiffness constant \widehat{R}_y .

We also note that the SH waves are able to detect the reduction of the stiffness of the adhesive layer and therefore can be used for inspection of bonded joints. Although the SH waves are difficult to excite, some techniques using guided SH waves for nondestructive evaluation have been reported (Hirao, and Ogi, 1999).

5. Conclusions

The quasi-static approximation was used to model the adhesive layer of two aluminum bonded plates to simulate the propagation of Lamb waves and SH waves. The frequency spectrum and the dispersion curves of Lamb waves and SH waves were determined for different conditions of the adhesive layer by changing the stiffness constants of the springs. Comparisons among the dispersion curves for the perfect adhesion and the dispersion curves for deficient conditions of the adhesive layer, shown that the Lamb modes and the SH modes are sensitive to the alterations of the adhesive. We noted that the Lamb modes change accordingly with the stiffness constant modified. In the case of SH waves only the anti-symmetric modes change with the reduction of the stiffness constant. We also verified that in general, the phase velocity decreases when the stiffness constant of the springs are reduced.

With the widespread use of the adhesive bonding and the lack of adequate nondestructive testing procedures, the results of this work shown that the inspection techniques based on guided waves have a great potential for the evaluation of bonded joints.

6. References

- Achenbach, J.D., 1975, Wave propagation in elastic solids, North Holland, Amsterdam.
- de Barros, S.R., 2001, "Propagação de ondas SH e ondas de Lamb em placas coladas", dissertação de mestrado apresentada em 10 de agosto de 2001 no Depto. de Eng. Mec. da UFF.
- Baik, J.M. and Thompson, 1984, "Ultrasonic Scattering from imperfect interfaces: a quasi static model", J. Nondestructive Evaluation, 4, 177-196.
- Graff, K.F., 1991, Wave motion in elastic solids, Dover Publications.
- Guyott, C.C.H. and Cawley, P., 1988, "The ultrasonic vibration characteristics of adhesive joints", J. Acoust. Soc. Am. 83(2), pp.632-640.
- Heller, K., Jacobs, L.J., Qu, J., 2000, "Characterization of adhesive bond properties using Lamb waves", NDT&E, 33, pp. 555-563.
- Hirao, M. and Ogi, H., 1999, "An SH-wave EMTA technique for gas pipeline inspection", NDT&E International, 32, 127-132.
- Jones, J.P. and Whittier, J.S., 1967, "Waves at flexibly bonded interface", J Appl. Mech, p.905-908.
- Kundu, T., and Maslov, K., 1997, "Material Interface Inspection by Lamb waves", Int. J. Solids Structures, 34, 3885-3901.
- Lavrentyev, A. I. and Rokhlin, S.I., 1998, "Ultrasonic spectroscopy of imperfect contact interfaces between a layer and two solids", J. Acoust. Soc. Am. 103(2), pp. 657-664.
- Maslov, K. and Kundu, T., 1997, " Selection of Lamb modes for detecting internal defects in composite laminates", Ultrasonics, 35, 141-150
- Monkhouse, R.S.C., Wilcox, P W., Lowe, M.J.S., Dalton, R.P. and Cawley, P., "The rapid monitoring of structures using interdigital Lamb wave transducers", 4th ESSM and 2nd MIMR conference, Harrogate, pp. 397-404, 1998.
- Mustafa, V., Chahbaz, A., Hay, D.R., Brassard, M., Dubois, S., 1997, "Imaging of Disbond in Adhesive Joints with Lamb Waves", NDTnet.
- Pecorari, C. and Kelly; P.A., 2000, "The quasistatic approximation for a cracked interface between a layer and a substrate", J. Acoust. Soc. Am. 107(5), pp. 2454-2461.
- Singher, L., Segal, Y., Segal, E. and Shamir, J., 1994, "Considerations in bond strength evaluation by ultrasonic guided waves", J. Acoust. Soc. Am. 96(4), pp. 2497-2505.
- Xu, P.C., and Datta, S.K., 1990, "Guided waves in a bonded plate: A parametric study", J. Appl. Phys. 67(11), pp. 6779-6786.